Impact Effects on Meteoroid Shielding Configurations for Velocities up to 60,000 fps

F. C. Posever,* F. L. Rish,† and C. N. Scully‡
North American Aviation, Inc., Downey, Calif.

Cratering and penetration data were obtained experimentally with intact, spherical, borosilicate glass projectiles 48 μ in diameter at velocities from 20,000–60,000-fps in a hypervelocity gun facility. A relatively close correspondence at high velocities exists between Bjork's theoretical penetration results and the empirical logarithmic law proposed by Herrmann and Jones. Empirical constants for the logarithmic law are presented for steel, Al, Mg, and Be target materials. The equations, combined with an appropriate meteoroid mass-flux distribution and impact probability, suggest that current protective requirements against the meteoroid hazard might be reduced. Results for velocities between 16,000 and 38,000 fps give values near 1.5 for the ratio of the thickness of a single sheet, which is just perforated to the depth of a crater in a thick target. Data obtained from equal-thickness, two-sheet configurations spaced 0.125 in. apart tend to define a velocity region above and below which perforations are not obtained. The perforation velocity region is interspersed with nonperforation data points, indicating the need for a statistical approach to determination of ballistic limits for multiple-sheet shielding configurations.

Nomenclature

A = vulnerable area
$\bar{c}$ = longitudinal bar sonic velocity of the target material
d = diameter of projectile
e = base of natural logarithms
$F_>$ = flux or frequency of particles with mass equal to or greater than m
H = Brinell hardness number
k = constant
m = projectile mass
N = number of penetrations
$\bar{N}_>$ = average number of impingements of particles with masses greater than or equal to m
p = depth of penetration measured from plane of original surface
$P(N)$ = probability of N penetrations
V = projectile impact velocity
α = environmental constant
β = environmental exponent for mass
γ = penetration coefficient
θ = exponential parameter for Mach number, $V/\bar{c}$
ρ = density
τ = environmental exposure time interval
ϕ = exponential parameter for density ratio, ρ_p/ρ_t

Subscripts

p = reference to particle or projectile
s = reference to shield
t = reference to target
T = reference to witness plate
∞ = reference to quasi-infinite target

Introduction

THE success of manned space flights depends to a large extent on the adequacy of protection against meteoroids. This paper describes some results of an experimental hypervelocity impact program involving multiple-sheet shielding configurations.

The Mark IV hypervelocity gun at the Space and Information Systems Division (S & ID) Space Sciences Laboratory is schematically represented in Fig. 1. It is electrically energized by a series of special low-inductance, high-voltage capacitors that discharge in an arc chamber containing lithium. The release of energy generates a high-temperature lithium plasma that flows through a nozzle to an evacuated flight range, thus accelerating a large number of spherical projectiles through the nozzle by plasma-flow drag forces. The projectiles pass through a series of baffles that intercept all particles not collimated with the flight-range axis. The relatively few remaining projectiles traverse light-scattering and velocity sensors and strike the target. Reference 11 describes the gun in greater detail. Improvements in gun design during the course of experimentation increased velocity capabilities up to 65,000 fps.

In all of the experiments, cratering and perforation data were obtained with intact, spherical, borosilicate glass projectiles 0.0019 in. (49 μ) in diameter. The number of projectiles loaded for a single firing is on the order of several thousand particles, but relatively few survive passage through the system of baffles. The uniformity of projectile diameters, therefore, is initially controlled and maintained within close tolerances. Particle integrity (intactness) was determined by means of a light-scattering sensor prior to impact. Aluminum, magnesium, and steel alloys and beryllium were used as target materials. The target configurations included quasi-infinite plates, thin sheets (0.4 to 2.5 mils thick) in one-, two-, and three-layer configurations, and sandwich composites using hexagonal aluminum honeycomb and polyurethane fillers.

Determination of Particle Integrity and Velocity

Particle intactness during flight is verified periodically by means of the light-scattering sensor. A highly uniform, intense light source illuminates the projectiles which are sensed by a photomultiplier. The location of the photomultiplier

Table 1 Experimentally determined exponents

Material	ϕ	θ	k_1	k_2
Aluminum	4.52	1.136	0.854	37.5
Steel	1.03	0.902	0.511	69.4

Presented at AIAA Fifth Annual Structures and Materials Conference, Palm Springs, Calif., April 1–3, 1964 (no preprint number; published in bound volume of preprints of the meeting); revision received November 2, 1964. This study was conducted for the Aeronautical Systems Division, U. S. Air Force, under Contract No. AF 33(657)-8159.

* Research Specialist, Aerospace Sciences, Space and Information Systems Division.

† Supervisor of Structural Sciences, Aerospace Sciences, Space and Information Systems Division. Member AIAA.

‡ Scientist-Space Research, Space Sciences Laboratory, Space and Information Systems Division.

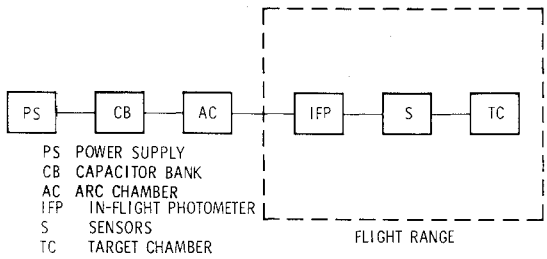

Fig. 1 Schematic diagram of Mark IV hypervelocity gun.

excludes direct radiation from the source, and only radiations from the particle are detected. The intactness of projectiles is determined by comparison of the signal amplitude received by the sensor with a plot of signal amplitude vs particle size obtained from firings with compressed air in which particle integrity is assured. A single-sweep oscillogram obtained from two intact spherical particles and one fragmented particle is shown in Fig. 2. In addition, particle intactness is determined during gun performance checks in which firings are made on 1100 F aluminum targets. The penetrations obtained during the performance checks are compared to 1100 F aluminum data plots of p_∞/d vs velocity, based on a high confidence set of 77 impacts, to determine particle intactness.

The time of flight interval is triggered by capacitor discharge and recorded on oscillograms that can be read within 5 μsec. The acceleration interval in the nozzle is approximately 5 μsec. The distance from nozzle to target is 3690 $\pm$ 5 mm for the quasi-infinite target experiments and 3740 $\pm$ 5 mm for two-sheet and three-sheet targets. Velocities, with maximum errors of approximately 2.5% at high values and less at lower values, are determined from the simple time-distance relationship. The impacts shown in Fig. 3 occurred at velocities of 53,800 and 46,000 fps. The initial transient, caused by inductive electrical noise during arc discharge, is difficult to shield against and appears on all records.

Schedule of Experiments and Results

In general, the experiments were sequenced to provide a maximum of information that could be used to design target specimens for subsequent tests. Quasi-infinite targets of Al, steel, Mg, and Be were impacted in that order primarily to verify impact behavior of the basic materials, uninfluenced by the effects of target thickness, and to establish a basis from which the single-sheet target thicknesses could be determined. The collection of quasi-infinite data was programed to obtain best-fit curves on both log-log and semi-log plots of the penetration parameter p_∞/d vs velocity. The results of the semi-log plots are presented in Fig. 4, which shows points, representing groups of data points, that indicate the experimental scatter. The results for Al and steel are well defined by the curves, but the Mg and Be data tend to scatter more widely. The mechanical and physical properties of the target samples of Be are unknown and were not determined during the present program. The penetration

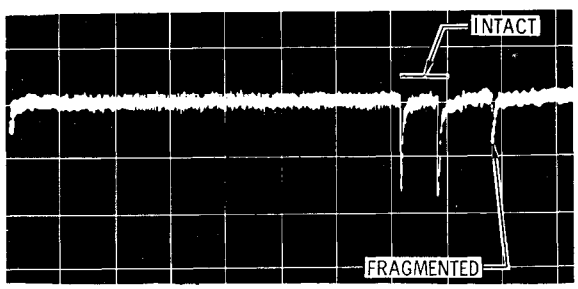

Fig. 2 Light-scattering sensor oscillogram showing two intact particles and one fragmented particle.

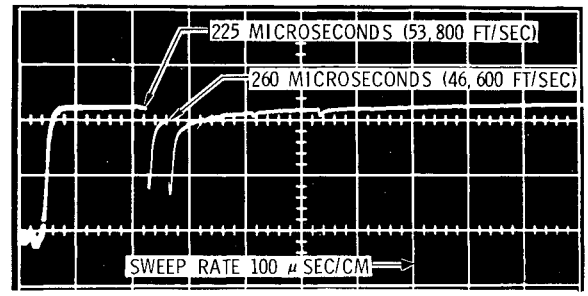

Fig. 3 Oscillogram of hypervelocity impact flash.

equations obtained are as follows:

$$\text{Al:}\quad p_\infty/d = -12.8 + 3.21 \log_{10} V$$

$$\text{Mg:}\quad p_\infty/d = -14.4 + 3.60 \log_{10} V$$

$$\text{Be:}\quad p_\infty/d = -16.1 + 3.84 \log_{10} V$$

$$\text{Steel:}\quad p_\infty/d = -6.52 + 1.67 \log_{10} V$$

With respect to depth of penetration, steel is superior not only to Mg and Al, but also to Be over a significant range of velocities. Using single-sheet perforation thickness to obtain the weight per unit area perforated ρt_s, the materials may be ranked as follows: 1) Be (lightest), 2) Mg, 3) Al, and 4) steel.

The empirical equations developed by Charters and Summers[1,2] and those of Herrmann and Jones[3] were fitted to the quasi-infinite data in the velocity range between 25,000 and 40,000 fps. The Charters and Summers equation was developed from early experiments with lead and copper at relatively low velocities using both a powder gun and a piston-compression light-gas gun. It can be expressed in the following general form:

$$p_\infty/d = \gamma(\rho_p/\rho_t)^\phi\,(V/\bar{c})^\theta \qquad (1)$$

Using a value of 2.0 for γ, the experimental data produced values of the exponential parameters ϕ and θ shown in Table 1.

Herrmann and Jones examined a large body of existing experimental data and found good correlation with an expression of the following form:

$$p_\infty/d = k_1 \log_e[1 + (\rho_t V^2/k_2 H_t)] \qquad (2)$$

The constants k_1 and k_2, which are dependent upon the projectile and target materials, were determined empirically from data for many projectile target material combinations;

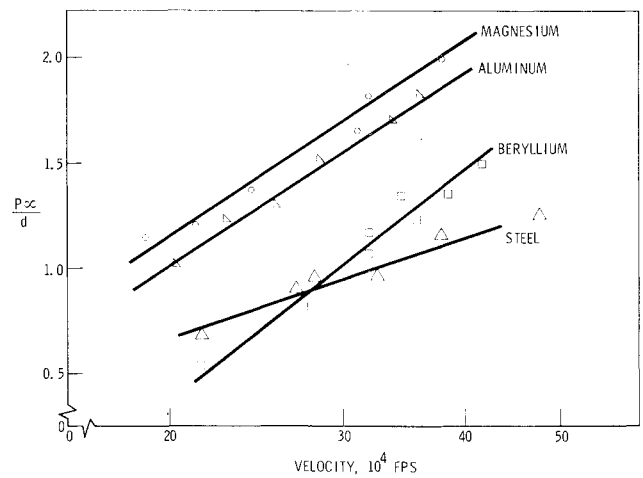

Fig. 4 Hypervelocity impact test results for quasi-infinite targets; projectile: borosilicate glass (0.0019-in.-diam spheres)

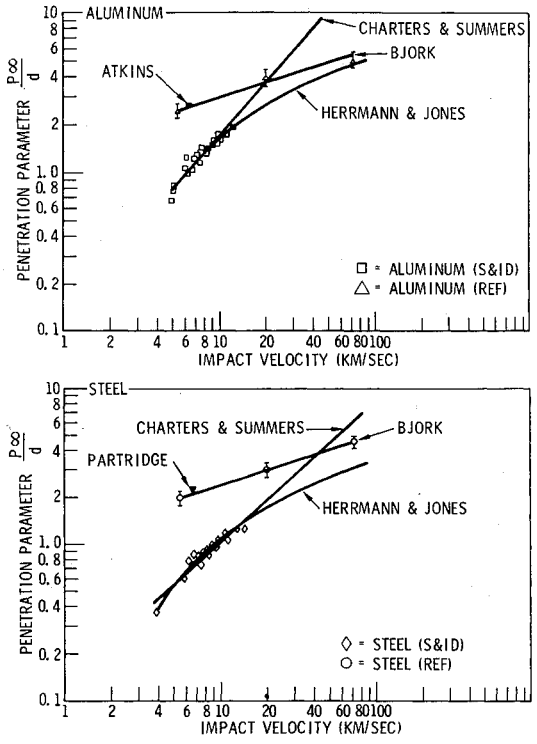

Fig. 5 Penetration parameters for quasi-infinite targets as a function of impact velocity (aluminum and steel).

the values for Al and steel impacted by borosilicate glass projectiles are shown in Table 1.

Herrmann and Jones observed that the empirical logarithmic law compared favorably with Bjork's theory at high velocities. Maiden[4] compared data points obtained at velocities up to 9 km/sec for aluminum projectiles impacting aluminum targets with empirical equations of several investigators, including Herrmann and Jones, and Bjork's theoretical results. The quasi-infinite data fits, using the Charters and Summers and the Herrmann and Jones equations along with some results of other investigators, are compared with Bjork's theory[5,6] in Fig. 5. The correspondence between the data from Maiden, Herrmann and Jones, and Bjork is remarkable. Similarly, considering the effects of brittle projectile behavior from which smaller penetrations should be expected, the correspondence with the present data is no less remarkable.

Kinard et al.[7] related penetrations produced in quasi-infinite targets to perforations of single sheets; the single-sheet thickness of the target t_s was found to equal 1.55 p_∞. Olshaker[8] obtained data for lead projectile impacting lead targets at 8200 fps. The mechanism of penetrations in lead at this velocity was assumed to simulate "fluid impact"

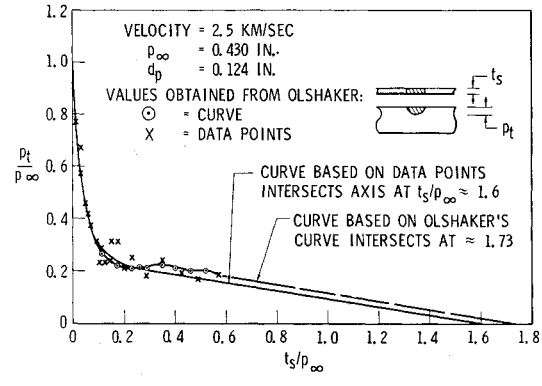

Fig. 6 Plot of p_T/p_∞ vs t_s/p_∞ from Olshaker's data for lead impacting lead.

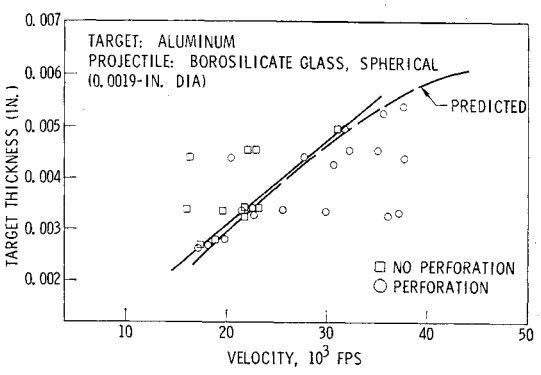

Fig. 7 Ballistic limit for single-sheet targets (S&ID data)

penetration in structural materials. The data appear (in terms of present nomenclature) as a plot of t_s/d_p vs $(t_s + p_T)/p_\infty$. The values of t_s/p_∞ and p_T/p_∞ were calculated and are replotted as shown in Fig. 6. Extrapolation of the data curve to $p_T/p_\infty = 0$ produced a value of the ratio of single-sheet perforation to quasi-infinite target penetration t_s/p_∞ approximately equal to 1.6.

A value of 1.5 for the penetration coefficient, along with S&ID data from quasi-infinite target experiments, was used to approximate the single-sheet target thicknesses for the perforation experiments conducted at S&ID. The predicted perforation thicknesses shown in Fig. 7 for aluminum were in excellent agreement with experimental results. The approximation of 1.5 for the penetration coefficient was supported by the experiments at least up to velocities of 40,000 fps.

The data obtained from equal-thickness, two-sheet configurations spaced 0.125 in. (62.5 particle diameters) apart appear in Fig. 8. The total thicknesses of front and back sheets for these experiments ranged from 1 to 3.5 mils, and the velocities ranged from 6000 to over 60,000 fps. A combined total of 112 shots supplemented by valid two-sheet results from three-sheet experiments were recorded. Over the domain of thicknesses involved, the data define a velocity region above and below which perforations are not obtained, as indicated by the dotted curve. The perforation barrier established by these data is interspersed with nonperforation data points. Nevertheless, support for the following implications is established: 1) severe particle fragmentation occurs over the domain of thicknesses tested; 2) particle fragmentation occurs randomly; 3) thin front sheets are sufficient to induce severe particle fragmentation; 4) at least up to velocities of 60,000 fps, a second perforation barrier does not exist.

The first three implications lead to the familiar "bumper" concept proposed by Whipple.[9] The fourth partially answers the question regarding multiple-sheet meteoroid shielding behavior at higher velocities. In addition, following the line established by a definition of the ballistic limit for a given projectile, target, and spacing (i.e., the velocity at which 50% of the impacts perforate), a statistical approach to solving the mechanics of multiple-sheet perforations is indicated and currently is being pursued.

In summary, the impact data on aluminum and steel show that the crater depths produced in thick targets by borosilicate

Table 2. Constants for several suggested mass-frequency distributions of meteoroids

Environment	α, gm/cm²-sec	β
Suggested near-earth omnidirectional flux	0.11×10^{-16}	1.0
Maximum lunar surface hemispherical flux	0.63×10^{-17}	1.0
Minimum lunar surface hemispherical flux	0.24×10^{-17}	1.0

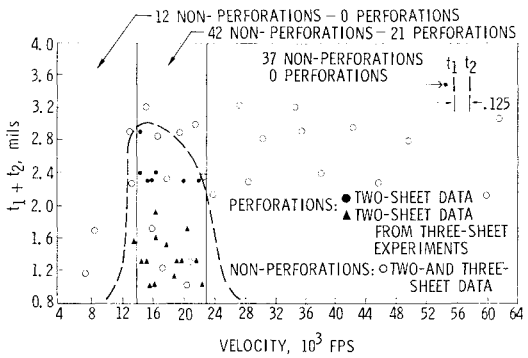

Fig. 8 Hypervelocity perforation for two-sheet configurations of aluminum (representing 112 data points)

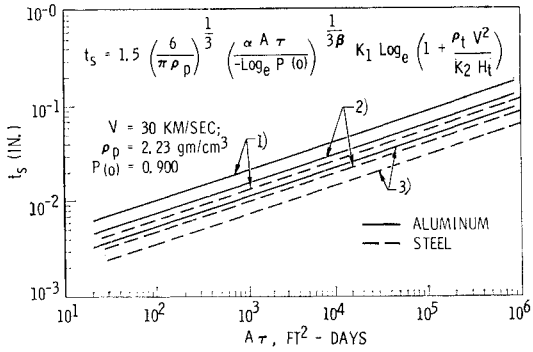

Fig. 9 Single-sheet shield thickness t_s vs. exposure parameter ($A\tau$) for several suggested meteoroid environments: 1) based on suggested near earth omnidirectional flux, 2) based on maximum lunar surface hemispherical flux, 3) based on minimum lunar surface hemispherical flux.

glass projectiles, which represent the density of the more numerous particles of the meteoroid population in space, are correspondingly smaller than those produced by metallic particles. Combining the other facts established during the course of the experimental program with a near-earth cumulative mass frequency distribution of meteoroids in space, an engineering evaluation can be made for single-sheet protective shields.

A general relationship for near-earth cumulative mass frequency distribution of meteoroids may be expressed as $F_> = \alpha m^{-\beta}$ where $F_>$ is the flux or frequency of particles with mass equal to or greater than m, and α and β are constants obtained empirically. Unpublished estimates of the Flight Sciences Department of S&ID for α and β, within present limits of knowledge and applicable in the range 10^{-4} gm $< m <$ 2.5 gm, are shown in Table 2.

For a vulnerable area A and an exposure time τ, the average number of impingements of particles with masses greater than or equal to m is $\bar{N}_> = F_> A\tau = \alpha m^{-\beta} A\tau$.

The mass m may now be substituted in Eq. (2) for the particle parameter d. Since the particle is spherical, $d = (6m/\pi\rho_p)^{1/3}$ where ρ_p is the density. Using $\beta = 1$, from the relation $\bar{N}_> = \alpha m^{-1} A\tau$ we get $m = \alpha A\tau/\bar{N}_>$. For the probability of occurrence of a specified number of penetrations per unit of time, in the absence of sufficient empirical information, the presently accepted approach employs the mathematical Poisson model.[10] In terms of the average number of penetrations $N_>$, the probability $P(N)$ of N penetrations is

$$P(N) = (1/N!)[(\bar{N}_>)^N (e)^{-\bar{N}_>}]$$

Setting requirements for no penetrations, we get

$$P(0) = e^{-\bar{N}_>} \text{ or } \log_e P(0) = -\bar{N}_>$$

By substituting these values, we get the relationship

$$t_s = 1.5\left(\frac{6}{\pi\rho_p}\right)^{1/3}\left(\frac{-\log_e P(0)}{\alpha A\tau}\right)^{-1/3} k_1 \log_e\left(1 + \frac{\rho_t V^2}{k_2 H_t}\right)$$

Using the information obtained from the experiments, a plot of t_s vs $A\tau$ (Fig. 9) was obtained. Comparison of the values of t_s taken from this curve with values taken from similar published curves shows that the former are definitely smaller. Coupled with the higher probability of occurrence of oblique impact effects, also associated with smaller penetrations, the data obtained on the program suggest that current protective requirements against the meteoroid hazard in space might be reduced.

References

[1] Charters, A. C. and Locke, G. S., Jr., "A preliminary investigation of high-speed impact: The penetration of small spheres into thick copper targets," NACA Research Memo. A58B26 (1958).

[2] Summers, J. L. "Investigation of high-speed impact: Regions of impact and impact at oblique angles," NASA TN D-94 (1959).

[3] Herrmann, W. and Jones, A. H., "Survey of hypervelocity impact information," Massachusetts Institute of Technology Aeroelastic and Structures Research Lab. Rept 99-1 (1961).

[4] Maiden, C. J., "Meteoroid impact," General Motors Defense Labs. Tech. Memo 63-203 (1963).

[5] Bjork, R. L. *Effects of a meteoroid impact on steel and aluminum in space*, Rand Corp. Rept. P-1662 (1958).

[6] Bjork, R. J. "Meteoroids versus space vehicles," ARS J. **31**, 803–807 (1961).

[7] Kinard, W. H., Lambert, C. H., Jr., Schryer, D. R., and Casey, F. W., Jr., "Effect of target thickness on cratering and penetration of projectiles impacting at velocities to 13,000 feet per second," NASA Memo. 10-18-58L (1958).

[8] "Fourth hypervelocity impact symposium," Air Proving Ground Center, APGC-TR-60-39 (II), sponsored by U. S. Army, Navy, and Air Force (1960).

[9] Whipple, F. L., *Meteoroitic Phenomena and Meteorites, Physics and Medicine of the Upper Atmosphere*, edited by C. S. White and O. O. Benson (University of New Mexico Press, 1952).

[10] Rodriguez, D. "Meteoroid shielding for space vehicles," Aerospace Eng. **19**, 20–23 (1960).

[11] Scully, C. N., Escallier, E. A., Rosen, F. D., and O'Keefe, J. D., "Electrothermal gun for hypervelocity ballistics research," *Proceedings of the Seventh Hypervelocity Impact Symposium* (1965). Vol. I, pp. 147–185.